esa

ECOSPHERE

Confirming a plant-mediated "Biological Tide" in an aridland constructed treatment wetland

Paul Bois,[1,2] Daniel L. Childers,[3,†] Thomas Corlouer,[2] Julien Laurent,[1,2] Antoine Massicot,[2] Christopher A. Sanchez,[3] and Adrien Wanko[1,2]

[1]*ICube (UMR 7357 ENGEES/CNRS/Unistra), 2 rue Boussingault, 67000 Strasbourg, France*
[2]*LTSER France, Zone Atelier Environnementale Urbaine, 3 Rue de l'Argonne, 67000 Strasbourg, France*
[3]*School of Sustainability, Arizona State University, Tempe, Arizona 85287 USA*

Citation: Bois, P., D. L. Childers, T. Corlouer, J. Laurent, A. Massicot, C. A. Sanchez, and A. Wanko. 2017. Confirming a plant-mediated "Biological Tide" in an aridland constructed treatment wetland. Ecosphere 8(3):e01756. 10.1002/ecs2.1756

Abstract. As urban populations grow and the need for sustainable water treatment increases, urban constructed treatment wetlands (CTWs) are increasingly being used and studied. However, less is known about the effectiveness of this "turquoise infrastructure" in arid climates. In a recent publication, we presented evidence of plant-mediated control of surface hydrology, using a water budget approach, in a CTW in Phoenix, Arizona, USA. We also demonstrated how this transpiration-driven wetland surface flow made this treatment marsh more effective at pollutant removal than its counterparts in cooler or more mesic environments. Water budget-based calculations estimated that nearly 20% of the water overlying the marsh was transpired daily by the plants (40–60 $L \cdot m^{-2} \cdot d^{-1}$) during the hottest summer months. We estimated the associated water velocity to be about 40 cm/h. In this paper, we report on hydrodynamic experiments that confirmed the existence of this phenomenon that we refer to as the "Biological Tide," and verified the rate at which transpiration by the marsh vegetation moves surface water into the biogeochemically active marsh. We combined a water budget-based approach and dye tracer experiments to quantify and confirm this phenomenon. Because of the low velocities estimated from our water budget approach (a few cm/h), we used a fixed-wall flowthrough marsh flume to limit the lateral dye movement during the tracer experiments. We measured actual flow rates of 7–50 cm/h (with 5–8% precision) during these experiments, which closely conformed to the values estimated from our water budget-based approaches. The flow was largely dispersive due to the extensive impedance imparted by dense plant stems in the marsh. From these summer flow rates, we calculated that residence time of the water overlying the marsh in this CTW averaged about 13 d, but could be as low as four days. Again, these values were reasonably close to the 15–20% replacement rate for marsh water we estimated using the water budget approach. This is the first time, to our knowledge, that plant-mediated biological control of surface hydrology in a wetland, without connection to groundwater, has been reported.

Key words: constructed treatment wetland; dye tracer experiment; ecological engineering; transpiration; urban sustainability; wastewater treatment.

Received 14 December 2016; revised 13 February 2017; accepted 13 February 2017. Corresponding Editor: Ryan A. Sponseller.

† **E-mail:** Dan.childers@asu.edu

Introduction

Humans are becoming an increasingly urban species: Since 1900 the proportion of people living in cities has increased from 10% to over 50% globally, and will likely be 80% by 2050 (Grimm et al. 2008). In the last 100 yr, many cities have transformed into "sanitary cities," with highly centralized, capitalized, and expensive infrastructure designed to keep inhabitants healthy (Melosi 2000, Grove 2009). Often this infrastructure has imparted large systemic inertias on cities that hinder novel or transformative new solutions to growing problems (Childers et al. 2014). Still, there are many ways to design urban infrastructure so as to optimize key ecosystem services by using "design with nature" approaches that make cities more resilient and sustainable (Pickett et al. 2013). When these urban designs incorporate terrestrial ecological features, they are typically called "green infrastructure," while "blue infrastructure" refers to aquatic systems. One example of "designing with nature" is the increasing use of constructed treatment wetlands (CTWs) as part of urban wastewater treatment in place of expensive and energy-intensive treatment technologies. Wetlands have both terrestrial and aquatic ecological characteristics, and because of the color that results when green and blue are mixed, we refer to such urban wetlands as "turquoise infrastructure" (Childers et al. 2015).

Constructed treatment wetlands are a relatively low cost and low maintenance solution to urban wastewater and water reclamation challenges (Wallace and Knight 2006, Nivala et al. 2013). Most CTWs are designed to "polish" partially treated municipal effluent with a mix of open water areas, macrophytic vegetation, and waterlogged soils (Fonder and Headley 2013). Designs are often highly dependent on local or regional variables, including water quality regulations and site-specific conditions (Fonder and Headley 2010, Tanner et al. 2012), and rely on different flow types (subsurface [SSF] vs. free water surface [FWS] flow). While CTWs may be relatively similar in design and expectations, particular attention must be paid to the way these systems function in different climatic settings.

Arid environments make up more than 30% of the earth's land surface, and cities in these regions increasingly face water scarcity issues. To address these issues, many are turning to the reuse of treated municipal effluent for various urban uses (Greenway 2005), but the challenge is that reclaimed water used in densely populated areas must be clean. Notably, in the aridland city of Phoenix, Arizona, USA—where we conducted the research reported here—virtually all municipal effluent is reused (Metson et al. 2012), and the only real export of water from the city is to the atmosphere. Constructed treatment wetlands are a viable "design with nature" solution, but building these wetlands in hot, arid cities such as Phoenix may expose them to unique challenges associated with large losses of water via evaporation and plant transpiration. With this in mind, since summer 2011 we have been quantifying these water fluxes in a CTW operated by the City of Phoenix Water Services Department while also measuring wetland plant biomass and estimating the whole-system water and nutrient budgets (Sanchez et al. 2016, Weller et al. 2016). Our objective has been to understand the effect of atmospheric water losses on the whole-system water budget and on the ability of this CTW to remove nitrogen from wastewater effluent. We found large losses of water from the emergent marshes via plant transpiration during the hot, dry summer months—as much as 20–25% of the water overlying the vegetated marsh daily—and we identified a horizontal advection of surface water from nearby open water areas as the only way to replace this transpired water. We call this phenomenon a "biological tide" (hereafter Biological Tide; Sanchez et al. 2016), which is a different phenomenon from evapotranspiration-driven movements of shallow groundwater (White 1932, Bauer et al. 2004, McLaughlin and Cohen 2014). Transpiration-driven movement of shallow SSF water has been documented in a number of wetlands, including with tree islands in the Okavango Delta in Botswana (Bauer-Gottwein et al. 2007, Ramberg and Wolski 2008) and in the Florida Everglades (Bazante et al. 2006, Troxler-Gann and Childers 2006, Sullivan et al. 2014). However, to our knowledge, this is the first time that biotic control of surface hydrology has been demonstrated in any wetland. In this paper, we present data from two different approaches that independently corroborated this plant-driven movement of water into a CTW marsh, verifying that this unique, never-before-described phenomenon exists.

Furthermore, this plant-mediated Biological Tide is actually increasing the nutrient removal efficacy of the CTW we studied: The vegetated marsh consistently removed virtually all of the inorganic nitrogen (N) made available to it, despite high rates of transpirational water loss (Sanchez et al. 2016). By bringing additional water and solutes into the vegetated marsh and its soils, from adjacent open water areas, the Biological Tide actually enhanced the ability of the marsh to remove N relative to CTWs found in cooler or more mesic settings (Sanchez et al. 2016).

The objective of this work was to measure actual surface water flow within the marsh and to compare these flow rates to those estimated using our transpiration-based water budget calculations. Often water flow measurement experiments conducted in wetlands include the entire system or flow rates on the order of cm/s (Leonard and Luther 1995, Leonard and Croft 2006). In this case, though, the spatial scale of our experiment was small and the magnitude of expected velocities was very low—a few cm/h. These challenges required a different methodological approach. One of the easiest ways to measure water velocities is with a flowmeter, but this technique will not work at low flow velocities (~0.4 cm/s) because of inappropriate detection limits. Doppler velocimetry is an alternative, but Doppler flowmeters typically require a minimum water depth on the order of 0.25–0.5 m (Meselhe et al. 2004), and the water overlying vegetated wetlands is often shallower than this. Plant stems also interfere with the propagation of the acoustic signal, making Doppler results from vegetated wetlands difficult to obtain or analyze. In our CTW study site, water depths in the vegetated marsh averaged roughly 0.25 m, plant densities and productivity were high (Weller et al. 2016), and by our estimates, the Biological Tide flowed at only a few cm/h. Therefore, the only viable technique for documenting this flow was a tracer experiment.

The application of tracer studies to wetlands is not new (Bowmer 1987). Such tracer experiments have been used to calibrate hydrodynamic models of secondary and tertiary treatment wetlands (Giraldi et al. 2009, Laurent et al. 2015), to study on the effects of vegetation on flow dynamics (Bodin et al. 2012), to study internal wetland flows (Williams and Nelson 2011), and to examine the influence of water flow on CTW capacity (Worman and Kronnas 2005). Measuring water flow with tracers generally involves either direct water sampling or image recording. Either approach is relatively straightforward, and both are adapted to the low velocities that characterize vegetated environments (Meselhe et al. 2004). These very low flow rates create another complication, though: Lateral dispersion of the tracer may exceed directional advective–dispersive flow, decreasing our ability to longitudinally detect the tracer signal. To overcome this challenge, we added to our experimental design a fixed-wall flowthrough marsh flume to contain the dye tracking the Biological Tide flow within the vegetated marsh (for flume details, see Childers and Day 1988, 1990*a*, *b*, Childers 1994, Bouma et al. 2007, Harvey et al. 2011, Chang et al. 2015).

Methods

Site description

This work was conducted at a CTW associated with the largest wastewater treatment plant in Phoenix, Arizona, United States. We have focused our work on a 42-ha wetland that is part of this CTW, half of which is fringing vegetated marsh and half of which is mostly open water with several small upland islands (Fig. 1). The CTW is bounded by levee roads; it received from 95,000 to over 270,000 m^3/d of effluent, depending on the time of year. Water depths in the fringing marshes were consistently about 25 cm, while open water depths were 1.5–2 m; these depths did not vary because of the way water was managed in the system. The marshes were vegetated by seven emergent wetland species that are native to Arizona: *Typha latifolia, Typha domingensis, Schoenoplectus acutus, Schoenoplectus americanus*, *Schoenoplectus californicus, Schoenoplectus maritimus,* and *Schoenoplectus tabernaemontani* (Weller et al. 2016).

Plant transpiration measurements

We measured plant transpiration on a bimonthly schedule (January, March, May, July, September, and November), beginning in July 2011, using a LI-6400XT handheld infrared gas analyzer (LI-COR, Lincoln, Nebraska, USA). Leaf-level, plant-specific transpiration measurements were taken on individual *T. latifolia, T. domingensis, S. acutus, S. americanus, S. californicus*, and *S. tabernaemontani* plants along 10 transects evenly spaced

Fig. 1. Aerial image of the 42-ha Tres Rios constructed treatment wetland. White lines are the locations of the 10 marsh transects (each 50–60 m long), and blue arrows show the water inflow and outflow points. The star indicates where the July 2015 controlled-flow dye study was conducted.

around the fringing vegetated marsh, as well as along vertical (water surface to plant tip) and temporal (morning to afternoon) gradients (see Weller et al. 2016 for details on the experimental design). We used custom-made foam pads to create an airtight seal on the IRGA sampling chamber and to minimize plant damage when plant stems were thick or round, such as with *Schoenoplectus* plants. The IRGA also made measurements of ambient atmospheric conditions, including photosynthetically active radiation (PAR), air temperature, and relative humidity (see Sanchez et al. 2016 for sampling details).

We scaled these instantaneous leaf-level transpiration rates to whole-system transpiration volumes by relating the IRGA data to key whole-system datasets. Leaf-level transpiration rates were scaled across space with our bi-monthly estimates of whole-system species-specific macrophyte biomass (Weller et al. 2016, see *Plant biomass measurements* for more details). We used hourly meteorological data provided by the City of Phoenix, from an on-site meteorological station, to scale leaf-level transpiration rates in time, accounting for water losses when we were not sampling (Sanchez et al. 2016).

Transpirational water losses estimated since summer 2011 followed a strong seasonal pattern, with the greatest rates in July, when plant biomass, air temperature, and PAR were at annual maxima (Sanchez et al. 2016, Weller et al. 2016). It would follow that the plant-mediated Biological Tide would thus be strongest during the summer. As such, we conducted this study in July of 2014 and 2015. We used a water budget approach to estimate the magnitude of the Biological Tide that involved estimating the total volume of water overlying the vegetated marsh, accounting for volume displaced by standing live plants, and comparing this to bi-monthly transpirational water losses from July 2011 through September 2015.

Plant biomass measurements

We used bi-monthly estimates of live plant biomass to scale our leaf-specific plant transpiration measurements to the entire 21 ha of marsh. To quantify whole-system biomass, we developed phenometric models that allowed us to non-destructively estimate live biomass for all plant species using simple allometric measurements made in the field (Daoust and Childers 1998, Childers et al. 2006). Every two months, we measured all of the plants in five 0.25-m^2 quadrats that were randomly located along each of the 10 marsh transects, for a total of 50 0.25-m^2 quadrats sampled (Weller et al. 2016). We used simple linear interpolation to extrapolate plant biomass between bi-monthly samplings, producing daily

estimates of live macrophyte biomass from July 2011 through September 2015. Because the phenometric biomass models were not statistically different for *T. latifolia* and *T. domingensis* or for *S. acutus* and *S. tabernaemontani*, we combined these pairs of species into two species groups for calculations and analysis (Weller et al. 2016).

Summer 2015 dye tracer experiment

The summer 2015 Rhodamine dye tracer experiment was centrally located in our 42-ha study area (see white star on Fig. 1). We temporarily installed a fixed-wall flowthrough flume (2 m wide, 16 m long, 0.5 m high; Fig. 2) in the marsh, oriented perpendicular to the marsh–water interface and located approximately 10 m into the vegetated marsh. The walls were made from clear high-gauge plastic sheeting with metal chain hemmed into the bottom edge to hold the walls against the soil surface. The walls were held up with PVC poles located every 2 m.

We deployed five autosamplers (ISCO 6700) close to the flume on an existing boardwalk (Fig. 3). Sampler tube intakes were installed in the center of the flume 1, 3, 5, and 7 m inland from the Rhodamine dye injection point. One-liter samples were collected by the autosamplers at approximate half-water depth (i.e., ~12 cm from the bottom) either every 30 min or every hour over two-day experimental runs. The amount of water collected in these samples was negligible relative to the volume of water in the flume. We used a 30-min sampling time interval for the 1-m location to enhance measurement resolution. Two dye experiments were run a week apart, which allowed all residual Rhodamine to dissipate between the experiments. In the first experiment, we used 5 g Rhodamine B dye tracer powder (Fisher Scientific, Bridgewater, New Jersey, USA), while in the second we used 1 g. We made 1 L dye solutions on site using Tres Rios water, and the dye was gently injected into the marsh water at the injection point (Fig. 3).

Sample preparation and fluorescence analysis

Concentrations of Rhodamine B dye are easily determined using excitation fluorometry. We analyzed all samples on a Fluoromax 4 fluorometer (Horiba, Kyoto, Japan) after first diluting all samples (field samples and calibration solutions) tenfold with distilled water to avoid sensor saturation. The pH of Tres Rios water was effectively neutral and was stable (7.3 $\pm$ 0.1 SE), minimizing this possible source of fluorescence variation (Smart and Laidlaw 1977). Excitation and emission wavelengths were determined by recording the optimal response curve on an excitation–emission wavelength scan; we used an excitation wavelength of 546 nm and an emission wavelength of 590 nm. We also controlled for any possible background fluorescence in ambient Tres Rios water (e.g., by dissolved organics) by running field water blanks.

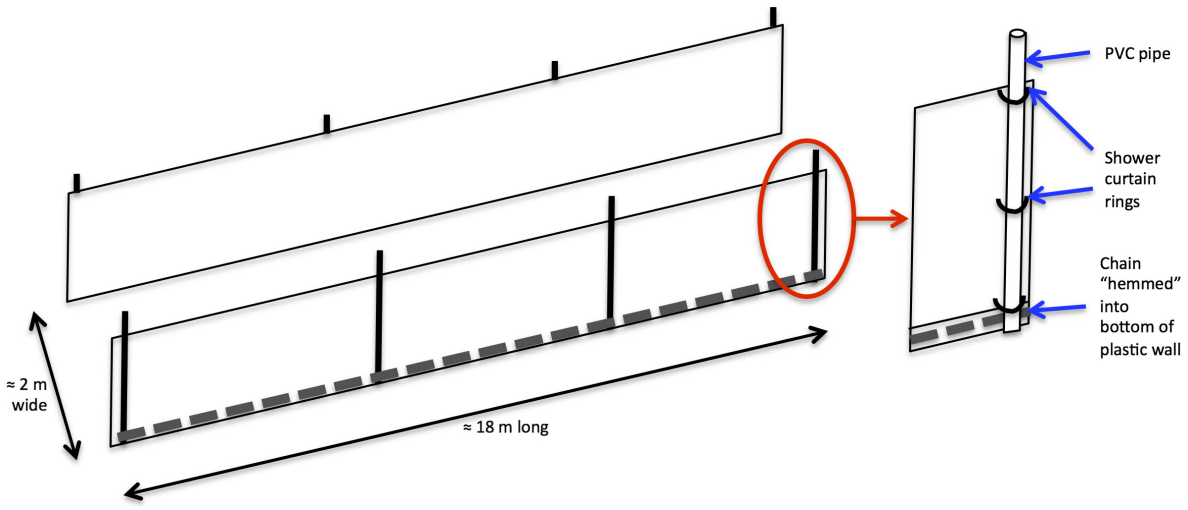

Fig. 2. Schematic of the temporary fixed-wall flowthrough marsh flume design, as modified from the approach used by Davis et al. (2001*a*, *b*).

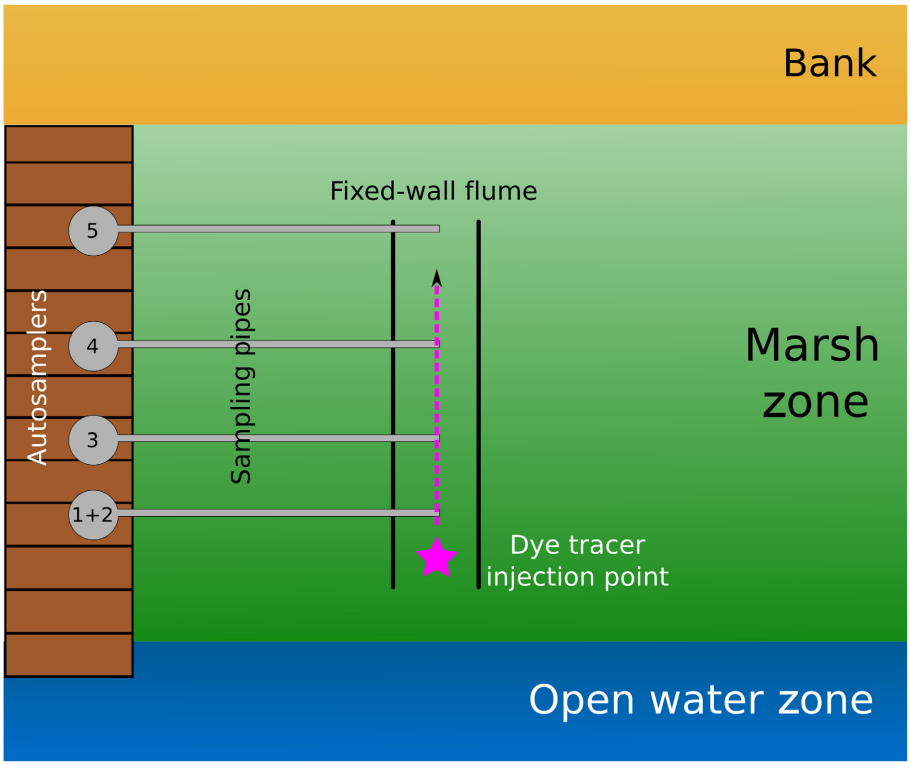

Fig. 3. Experimental design, including the approximate location of the 2 × 16 m flume (shown as "fixed-wall flume") adjacent to a boardwalk (left) and within the 50 m wide marsh. Sampling pipes allowed the autosamplers to collect water from within the flume without any disturbance of the marsh or soils during the experiment. The purple star indicates the dye tracer injection point.

Data analysis

We observed a low level of background fluorescence (due to the presence of dissolved organic matter), and we systematically accounted for it by subtracting the fluorescence values from the field water blanks from the sample signals. The resulting dye tracer breakthrough curves (BTCs) were used to compute residence time distribution (RTD) curves (Eq. 1, Table 1). The nth moments of the RTD curve ($\int_{t_0}^{t_f} E(t) \times t^n \times dt$) allowed us to subsequently determine the characteristics of the flow: The first moment ($n = 1$) corresponded to the mean residence time $\bar{t}$ (or MRT; Eq. 2, Table 1) and the second central moment ($n = 2$) corresponded to σ^2, where σ is the standard deviation (Eq. 3, Table 1).

We computed three different velocities:

1. The maximum velocity was based on the time when the first significant fluorescence signal appeared. It was computed as the ratio between the sampler position to the injection point and this first signal time of appearance. We calculated the associated precision with the time span between two samples (i.e., 0.5 or 1 h depending on the location);
2. The local mean velocity was computed as the ratio between the sampler position to the injection point and the mean residence time $\bar{t}$ (Eq. 4, Table 1);
3. The flume mean velocity was obtained by averaging the local mean velocities (when they could be computed) of the different sampling points for a given experiment.

Water displacement has three important characteristics: advection, dispersion, and diffusion. Advection is the global movement of the fluid particles due to the mean velocity. In cases where multiple flowpaths are possible, different velocities may result when different flowpaths are followed: This is dispersion. The third mechanism, diffusion, results from thermal movement

Table 1. Summary of the formulas and equations used.

Eq. no.	Parameter	Symbol	Unit	Formula
(1)	Residence time distribution	$E(t)$	h^{-1}	$E(t) = \frac{C(t)}{\int_{t_0}^{t_f} C(t) \times dt} \left(\int_{t_0}^{t_f} E(t) \times dt = 1 \right)$
(2)	Mean residence time	$\bar{t}$	h	$\bar{t} = \int_{t_0}^{t_f} E(t) \times t \times dt$
(3)	Standard deviation	σ	h	$\sigma = \sqrt{\int_{t_0}^{t_f} E(t) \times (t - \bar{t})^2 \times dt}$
(4)	Local mean velocity	$\bar{V}$	cm/h	$\bar{V} = \frac{\Delta X}{\bar{t}}$
(5)	Peclet number	Pe	–	$\frac{\sigma^2}{\bar{t}^2} = \frac{2}{Pe} + \frac{8}{Pe^2}$
(6)	Transpiration flow	Q_{ET}	m^3/h	$Q_{ET} = V_{ET}/t_{transpiration}$
(7)	"Biological Tide" velocity	$v_{Biological\ Tide}$	cm/h	$v_{Biological\ Tide} = Q_{ET}/S_{flow-through}$

Notes: t_0, starting time of the experiment. t_f, ending time of the experiment.

of molecules and is isotropic. For Rhodamine B, diffusion-induced displacement would be around 1 mm/h (Gendron et al. 2008) and was thus considered to be negligible in our case (see *Results*). To further characterize the flow within the marsh, we estimated the dispersive flow (Levenspiel 1998) by computing the Peclet number, a dimensionless number equal to the ratio of advective to dispersive flow ($Pe = (U \times L)/D$), where U and L are the typical velocity and magnitude of the flow, and D is the dispersion coefficient of the flow (Kadlec and Wallace 2009). The higher the Peclet number, the more advection dominates the flow (see *Results* section for the threshold values). The Peclet number can be computed from the value of the standard deviation σ (as defined above). The exact formulation of the equation linking the Peclet number and this variance depends on the boundary conditions of the experimental system —in this study, we used the formulation adapted to an open inflow–open outflow channel (Eq. 5, Table 1), which fits the flowthrough marsh flume that we used.

As we noted above, we ran two independent dye study experiments in July 2015, using the marsh flume. These were started at two different times: In the first, we injected the dye at 9 a.m. and the experiment ran for 24 h (Experiment 1), while the second was started at 4 p.m. and the experiment ran for 40 h (Experiment 2). These starting times were chosen to, respectively, cover day–night and night–day succession, in an attempt to differentiate any potential diurnal dynamics.

Velocities comparison

As an extension of our earlier work, we used our transpiration-based water budget to estimate Biological Tide water velocities in the marsh based on daily volumes of marsh water that must be replaced due to transpirational losses (Sanchez et al. 2016, Eq. 6, Table 1). We applied this same water budget approach to the 32 m^2 of marsh contained within our fixed-wall flume after measuring plant biomass and transpiration rates in the flume immediately after the dye experiments were completed. Using the flume cross section ($S_{flow\text{-}through}$), we estimated a Biological Tide water velocity $v_{Biological\ Tide}$ within the flume (Eq. 7, Table 1) using the same transpiration-based water budget approach. The Rhodamine dye measurements, however, were a direct measure of surface advective velocity ($v_{measured\ Biological\ Tide}$), which we compared with the two transpiration-based water budget estimates. Notably, the degree of coherence among these three independent flow rate values also served to validate our whole-system water budget calculations and estimates (sensu Sanchez et al. 2016).

Results

We adopted a three-pronged approach in this work, based on a whole-system water budget, a flume water budget, and a dye tracer experiment. In this part of the study, we will start by presenting the results of the global evapotranspiration measurements and the related Biological Tide calculations, subsequently converting them into hydraulic residence time and velocity. We will then present the calculations and results similarly obtained with the second approach. Finally, we will present the results of the dye tracer experiments, calculating velocities, and characteristic parameters of the flow.

Plant transpiration and Biological Tide calculations

Whole-system biomass and transpiration values for the study period (summer 2015) were consistent with annual and inter-annual trends that we have observed since July 2011, as reported in Sanchez et al. (2016) and Weller et al. (2016). Average aboveground biomass in July 2015 was 1462 ± 152 (SE) g dw/m^2. Across the 21-ha marsh, this equated to a total biomass of 332 MT dw (Fig. 4). *Typha* spp. was the dominant macrophyte across the wetland and at the site of our controlled-flow dye experiment; it represented 89% of the July 2015 biomass. The total whole-system plant transpiration in July 2015 was 194,580 m^3/month, or 2.7 cm/d (Fig. 4). While this was lower than the 343,760 m^3/month that we estimated for July 2011, these transpiration rates were still markedly higher than rates reported for wetlands in more mesic or temperate climates (Sanchez et al. 2016).

We calculated transpiration-based estimates of the magnitude of the Biological Tide phenomenon (Sanchez et al. 2016) as the fraction of water overlying the marsh that was lost every day via plant transpiration—and that thus needed to be replaced by surface water movement into the marsh from adjacent open water areas (Fig. 5). This renewal rate varied from 1% to 5% during colder winter months, when whole-system transpiration losses were approximately 500–1500 m^3/d, equivalent to 0.2–0.6 cm/d, to as high as 15–20% during the hot, dry summer months, when transpirational losses were 9000 to over 12,000 m^3/d, equivalent to 3.8–5.1 cm/d (Fig. 4). It follows that, in the summer, hydraulic residence times of water overlying the vegetated marsh were likely 5–6 d or less. Our marshes are roughly 50 m wide, so replacing 20% of the overlying water every day can be equated to a daily horizontal flow rate of about 10 m/d, or about 42 cm/h. We further note that these values are conservative, as they do not account for the volume of water displaced by extensive dead and thatched vegetation on the marsh. We did account for the volume of standing live plant stems that displace marsh water; without subtracting that stem volume, the volume of water overlying the marsh (to a mean depth of 0.25 m) would be 52,500 m^3.

We used this same transpiration-driven water budget approach to estimate flow rates within the 16 × 2 m fixed-wall flume, which held roughly 5.94 m^3 of water—maximal because we did not account for the displacement volume of

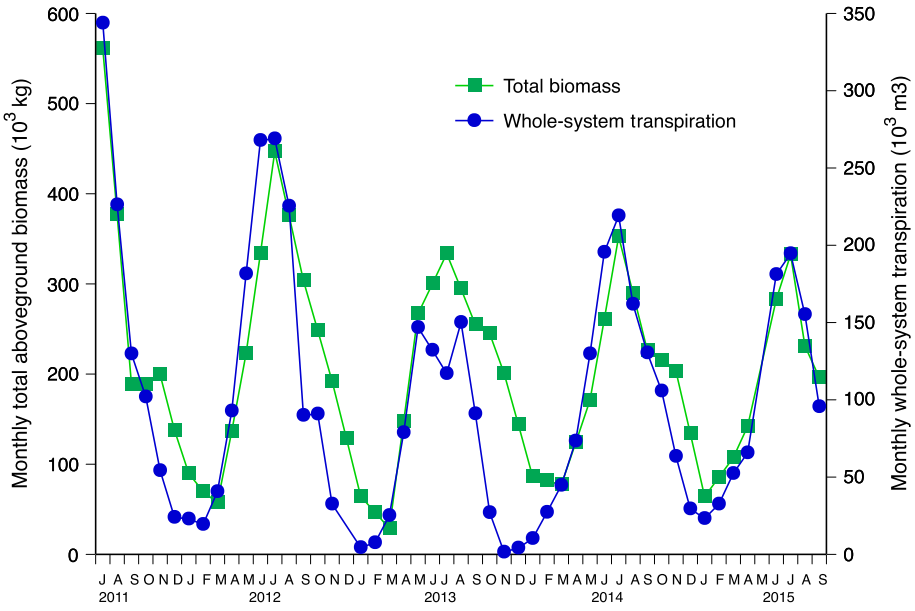

Fig. 4. Aboveground plant biomass and monthly total whole-system transpiration data from July 2011 through September 2015, including July 2015 when the controlled-flow dye experiment took place.

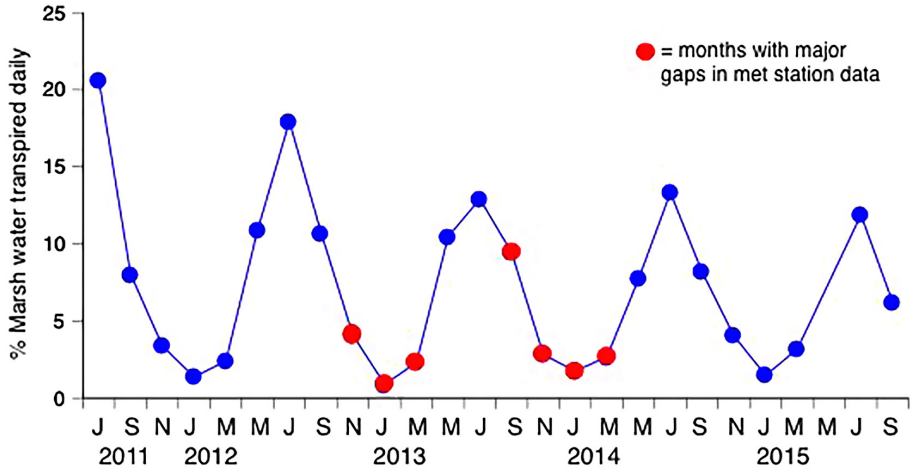

Fig. 5. Monthly average (±SE) fraction of the water overlying the marsh that was transpired daily from July 2011 through September 2015. Red circles represent months where transpiration was measured but could not be temporally scaled because of missing meteorological station data (see Sanchez et al. 2016 for details). Blue circles represent the percentage of marsh water transpired daily.

dead plant litter (wrack) or non-emergent aquatic vegetation (*Hydrocotyl* sp.). In July 2015, the 32 m^2 of marsh within the flume contained 30.3 kg dw of *Typha* sp. biomass that transpired 68 L/h (0.95 m^3/d or 3.0 cm/d) of water (taking into account 14 h of sunlight/d)—16% of the maximal volume of water within the flume. To replace this daily transpirational loss, new water would have had to flow into the flume at a rate of 2.57 m/d or 11 cm/h.

Dye experiments

Considering that (1) the water flow cross section within the flume was quite large compared with the tubing section of the autosampler and (2) the fixed walls of the flume were not impervious at the bottom, it was clearly very difficult to achieve a high tracer mass recovery. Neither a high recovery rate, nor the knowledge of the full RTD was the primary goal of this present work, though. We performed our calculations on the basis of the obtained BTCs (available in Appendix S1), which represent the fraction of the tracer mass we recovered. We got around 1% mass recovery for Experiment 1 and between 4% and 12% mass recovery (around 12% for the 1-m, 5% for the 3-m, and 4% for the 5-m sampling point) for Experiment 2. This low recovery rate had no impact on the data analysis in this study and the conclusions that are drawn, since the BTCs at the different sampling points gave valuable information.

For Experiment 1, we only calculated maximum velocity (see *Discussion*). For Experiment 2, the dye peak progressed down the flume in a predictable way, demonstrating that water was clearly, if slowly, advecting/dispersing into the marsh (Fig. 6). Additionally, the down-flume progression of the peak, from the marsh–open water interface toward the shore, confirmed the expected direction of water movement. In the first experiment, we calculated a high flow rate, 200 cm/h or 48 m/d, at the 1-m sampling location (Table 2). Otherwise, maximum velocities for both experiments ranged from 29 to 50 cm/h, or 7 to 12 m/d. The precision for these values was 5–8%. We found that the corresponding local mean velocities at the specific sampling points ranged from 7 to 25 cm/h (Table 2). The resulting flume mean velocity for this experiment was 16 cm/h, corresponding to 3.8 m/d.

In addition to advection, water flow is also characterized by dispersion and diffusion, and in low-flow situations where there are obstacles to flow—such as our marsh—dispersion may be a large component of flow. A simple measure of dispersion is the degree to which the fluorescence peaks widen and their tail increases with distance—and thus time—from the injection point. We found that the dispersion of the curves

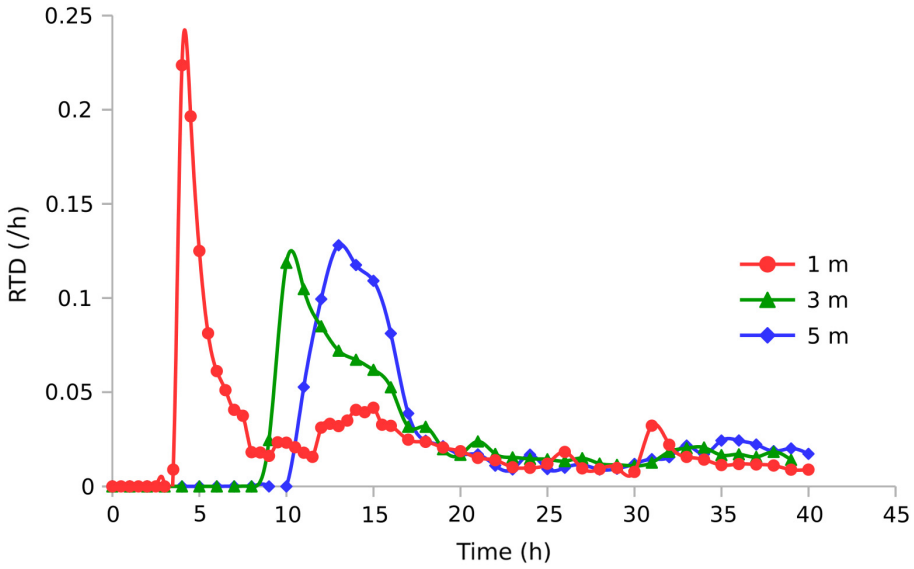

Fig. 6. Fluorescence curves for Experiment 2. Red circles (curve "1 m"), green triangles (curve "3 m"), and blue diamonds (curve "5 m"), respectively, represent the fluorescence at 1, 3, and 5 m from the injection point.

increased over distance (Fig. 6), demonstrating that the Biological Tide flow was (to a certain extent) dispersive. We were able to calculate Peclet numbers for only Experiment 2, because the calculation method required the use of the mean residence time, which we lacked for Experiment 1. One meter away from the injection point, the Peclet number was 6.2. Three and 5 m away from the injection point, its value was 12 and 13, respectively. As the characteristic length (L) and velocity (U) of the flow are 10 m and 16 cm/h (i.e., 4.4×10^{-5} m/s), the dispersion coefficient ($U \times L/\mathrm{Pe}$) for the flow ranges from 3.4×10^{-5} to 7.2×10^{-5} m^2/s. Finally, the recorded maximum velocities based on the fluorescence peaks observed at the 5-m sampling point were close to each other for both experiments (50 ± 2.8 and 45 ± 2.3 cm/h; Table 2), but not at the 1-m sampling point (200 and 29 ± 2.4 cm/h; Table 2). Based on these values, the difference between day to night (Experiment 1) and night to day (Experiment 2) flow rates were minimal, but additional experiments are needed to conclude this.

Discussion

We propose to compare the velocity of the Biological Tide with the velocities encountered in other wetlands, showing the relative magnitude of this phenomenon. We will then focus on the flow characteristics, especially its velocity range and dispersion features, providing comparison with the literature to situate the Biological Tide among the other types of flows already documented in

Table 2. Parameters calculated from the dye tracer experiments.

Experiment	Distance from injection point (m)	MRT (h)	Standard deviation σ (h)	Maximum velocity (cm/h)	Local mean velocity (cm/h)	Flume mean velocity (cm/h)	Peclet number (–)
1	1	na	na	200	na	na	na
	5	na	na	50 ± 2.8	na		na
2	1	15	11	29 ± 2.4	7	16 ± 5	6.2
	3	19	9	33 ± 2.1	16		12
	5	20	9	45 ± 2.3	25		13

Notes: MRT, mean residence time. Local mean velocity is defined as the ratio of the sampler position (i.e., distance from injection point) to the mean residence time for a given sampler (Eq. 3, Table 1). The flume mean velocity is defined as the average of all local mean velocities for a given experiment.

wetlands. A discussion about the relevance of the triple approach chosen in this study will follow, and we will conclude this part of the study by advancing management considerations involving comparison with wetlands displaying similar hydrodynamic features (namely velocity) or purposes (namely FWS CTW).

Marsh water velocity

The surface flow rates that we calculated from our July 2015 tracer experiments ranged from 29 to 45 cm/h. Using plant biomass and transpiration data from July, we estimated flow rates up to about 40 cm/h using our water budget approach. When we applied this same budget approach to the marsh within our 2 × 16 m fixed-wall flume, we calculated a conservative flow rate estimate of 11 cm/h. While these three independent approaches did not generate the same velocity, the estimates are reasonably close to each other and are thus believable. We found only one study where such low velocities have been reported: Kaplan et al. (2015) measured comparable surface flow velocities of 15–147 cm/h in a small (1.5 ha, 9000 m^3) vegetated tropical wetland that had an average water residence time of 90 d (Kaplan et al. 2011). By comparison, our Tres Rios CTW system was 42 ha in size—21 ha of which was vegetated marsh—held approximately 357,500 m^3 of water, and had a four-day design residence time. Our marsh surface flow velocities were much lower than those reported by Leonard and Luther (1995) for a tidal marsh in Florida—from 2 to 10 cm/s—although it is worth noting that tidal or gravity-based energy produced the currents in their tidal marsh, whereas plant transpirational water loss was the energy driving the Biological Tide in our CTW system. Regardless, there is considerable evidence that emergent vegetation in wetlands reduces both flow rates and turbulence (Leonard and Croft 2006).

The fluorescence value reached at the end of the Experiment 1 was too far from the baseline to compute the mean velocity value, unlike in Experiment 2. Indeed, the definition of a mean velocity implied that we were able to define the end point of the experiment (corresponding to the time when the fluorescence values return to background); this is a requirement to compute the MRT (Eq. 2, Table 1) and subsequently the local mean velocity (Eq. 3, Table 1).

The magnitude of the Biological Tide means that the renewing water will cover the marsh width (50 m) in approximately 13 d, based on the flume mean velocity (16 cm/h), but only 4.2 d for the fastest moving water parcels (50 cm/h). These maximum velocities (from 29 to 50 cm/h, Table 2) are the result of differential advective flow paths, characteristic of this dispersive flow. The Biological Tide is thus an advective–dispersive flow. The Peclet number was, in all cases, below the threshold value of 100 (Table 2), indicating that the flow we measured was largely dispersive (Levenspiel 1998). This can be explained by the high density and irregularity of plant stems within our marsh flume—almost 60% of flume surface and 2.4% of total water volume in the flume were occupied by live emergent plant stems—and more generally across the marsh. This leads to a multitude of possible flow paths for the water, which creates dispersion. This phenomenon has been documented in other wetland settings, including in other free surface water vegetated wetlands similar to our CTW (Keefe et al. 2004, Lightbody and Nepf 2006, Laurent et al. 2015). In our experiments, the dispersion coefficient ranged from 3.4×10^{-5} to 7.2×10^{-5} m^2/s, which is lower than previously encountered values: Coefficients between 1.3×10^{-4} and 6.3×10^{-4} m^2/s, 0.016 and 0.18 m^2/s, 2.5×10^{-3} and 2.1×10^{-2} m^2/s were, respectively, computed by Keefe et al. (2004), Variano et al. (2009), and Kaplan et al. (2015). This is most likely due to the lower velocities we observed in the Tres Rios marsh, as the Peclet numbers were quite similar among the aforementioned wetlands (respectively, around 30, 6–41 and 4–8).

The precision of our flow measurements ranged from 5% to 8%, which is reasonable for a field experiment under low velocity conditions. By comparison, the precision of most flowmeters and velocimeters is 2–20%. This precision and technical limitations (e.g., detection limit, measurement difficulty in a densely vegetated marsh) confirmed that a dye tracer experiment was the best way to measure the actual flow rates of the Biological Tide.

Comparison of transpiration-based water budget estimates and dye study results

We compared our water budget-based estimates of water replacement rates (Fig. 4) with water flow and replacement rates based on the

controlled-flow dye study conducted in July 2015 (Table 2). From transpiration calculations, we estimated a water velocity of 35–42 cm/h for a 50 m wide marsh in mid-summer, and a water residence time of 5–6 d for the water overlying the marsh (Fig. 5). The Rhodamine dye experiments confirmed velocities ranging from 25 cm/h (local mean velocity) to 45 cm/h (maximum velocity). The coherence between these two independent flow rate calculations is strong. As yet another methodological check, immediately after the dye experiment ended we also measured plant biomass and transpiration rates for the marsh within the 2 × 16 m fixed-wall flume itself, and used our water budget approach to estimate a replacement rate for the water in the flume. We estimated transpirational water loss within the flume area as roughly 950 L/d, or (a conservatively calculated) 16% of the total water volume within the flume. By extrapolation, we estimated that the rate of water flow that would be needed to replace this 16% loss, if the flume was closed at the downstream end, was 11 cm/h. This flume-specific water budget-based flow estimate is lower than, but still aligns reasonably well with, both our long-term whole-system transpiration-based estimates and the actual flow rates that we measured from the controlled-flow dye study.

Management considerations

Our five years of research at the Tres Rios CTW has documented that the most biogeochemically active zone of the system is the vegetated marsh (Sanchez et al. 2016, Weller et al. 2016). This is not surprising. But the management implications are important—if inorganic nitrogen, and presumably many other contaminants, gets into the marsh proper, they are effectively removed from the water (Weller et al. 2016). But the design water residence time for the entire 42-ha system, only 21 ha of which is vegetated marsh, is only four days, and it is likely that a considerable amount of the water entering the system leaves four days later without ever coming into contact with the biogeochemically active marsh. The high rates of summer water loss via plant transpiration, and the Biological Tide that is being driven by this, move more water and nitrogen into the marsh from the open water areas than would happen in a similar CTW in a cooler or more mesic climate. Thus, the biotically mediated surface hydrologic phenomenon that we have documented here, for the first time, is actually increasing the effectiveness of this CTW, simply because it is located in a hot, dry climate. Because of this, we would recommend a design for CTW in hot arid climates that either increases the relative area of vegetated marsh or increases the hydraulic likelihood that any given parcel of water in the system will come into contact with vegetated marsh.

Another design recommendation also focuses on water residence time. To demonstrate the potential importance of this hydraulic characteristic, we compared data from our CTW with similar values from a natural wetland located in the tropics (Costa Rica). The mean water residence time in natural La Reserva wetland was 100 d compared with 4 d in the Tres Rios CTW (Kaplan et al. 2011). This difference is largely because the water outflow rate at the latter was much higher (Table 3). One could expect that the higher water residence time in the La Reserva wetland would result in a higher nutrient uptake efficiency. However, the nitrogen removal efficiency of the La Reserva system (51–98.5%) was only double that of the Tres Rios CTW (22–48%, see Sanchez et al. 2016). If the Tres Rios CTW was designed for a longer whole-system water

Table 3. Comparison of hydraulic characteristics between a constructed treatment wetland (Tres Rios) and a natural wetland (La Reserva; Kaplan et al. 2011, 2015).

Parameters	TR	LR	TR/LR Ratio
Average outflow (m^3/h)	5000	6.25 ± 3.31†	523–1700
Volume (m^3)	351,500	7400–10,000†	35–48
Whole-system residence time (d)	4	30–110†	0.036–0.13
Marsh velocity (cm/h)	16	25–110‡	0.15–0.64
Marsh width (m)	50	–	–
Marsh residence time (d)	13	100†	0.13

Note: TR, Tres Rios wetland; LR, La Reserva wetland.

† Values from Kaplan et al. (2011). Intervals shown are 95% confidence intervals.

‡ Values from Kaplan et al. (2015). The lowest value corresponds to the wetland western average velocity; the highest one corresponds to the wetland eastern average velocity.

residence time, in conjunction with a physical design that allowed for more water contact with the vegetated marsh—and perhaps a higher marsh/open water ratio—we predict that its whole-system nutrient uptake efficiency, which is different from the marsh-specific uptake efficiency of nearly 100%, would be considerably higher.

Finally, in order to enlarge the comparison with systems sharing the same purpose and hydrological type, we put in perspective the removal efficiency of our wetland with a literature review of the removal performances of FWS CTWs (Kadlec and Wallace 2009). The reported mean removal rates reach 60% for ammonia, with a mean hydraulic loading rate of 7.3 cm/h (N = 118), and 46% for nitrate, with a mean hydraulic loading rate of 11.4 cm/h (N = 72). It thus appears that the Tres Rios CTW is fairly efficient, since the removal rates we measured reach 48% for ammonia and 22% for nitrate (Sanchez et al. 2016), while the hydraulic loading rate is roughly four times higher—42.9 cm/h. We can hypothesize that the Biological Tide we confirmed in the Tres Rios CTW, although not optimally utilized, already allows for significant nitrogen removal efficiency.

We are currently using a spatially articulate cell-based hydrodynamic model of the Tres Rios CTW, in conjunction with a biogeochemical processing model, to experiment with different hypothetical design options for this and other CTW systems.

Conclusions and next steps

We have used more than six years of data on plant community composition and biomass production, transpiration and evaporation rates, and water quality to verify the efficacy of nitrogen removal by the Tres Rios CTW. We have also used our whole-system water budget to demonstrate a plant-mediated, transpiration-driven Biological Tide that brings new water and nitrogen into the vegetated marsh of this CTW, where it is effectively removed and processed (Sanchez et al. 2016, Weller et al. 2016). In the research we present here, we used an empirical controlled-flow tracer study to confirm not only the existence and flow rates of the Biological Tide, but to verify the accuracy of our water budget-based estimates of flow rates. As we noted above, this is (to our knowledge) the first time that biotic control of surface hydrology has ever been demonstrated in a wetland ecosystem.

Our next steps involve using numerical modeling to further articulate how the Biological Tide phenomenon is enhancing nutrient removal in the wetlands of this CTW, and to explore design options for hypothetical CTW systems that optimize for this phenomenon. We are developing and parameterizing a spatially articulate hydrodynamic model, based on the current design of the Tres Rios CTW, that accounts for actual water flow rates between the marsh and open water bodies and that accurately simulates whole-system water residence times. We will then use this model to test various hypothetical design scenarios, including (1) different ratios and configurations of marsh and open water, (2) different open water flow paths, including a scenario where all water entering the system must come in contact with vegetated marsh, (3) various macrophyte community compositions, and (4) different plant densities (Kjellin et al. 2007). Ultimately, these modeling exercises will inform both improved management practices for the Tres Rios CTW and future designs that maximize the ecosystem services provided by CTW "turquoise" infrastructure in aridland cities around the world.

Acknowledgments

The first year of this work was supported by the U.S. Geological Survey through a grant from the Arizona Water Resources Research Institute. Additional support was provided by the National Science Foundation through the Central Arizona-Phoenix Long-Term Ecological Research Program (Grant No. 1027188) and the Urban Sustainability Research Coordination Network (Grant No. 1140070). The Walton Sustainable Solutions Initiative at ASU funded collaborative travel between Phoenix and Strasbourg, including P. Bois' travel in summer 2015. The Long-Term Ecological Research Network from France and the Strasbourg Long-Term Ecological Research Program (ZAEU) funded P. Bois' travel in summer 2014. We thank Hilairy Hartnett and Joshua Nye at ASU for the use of their fluorometer and lab space, Ben Warner for his contributions early in the project, Nich Weller for leading the macrophyte data collection efforts for the first three years of the project, the City of Phoenix Water Services Department for their support and for providing access to Tres Rios and key datasets, Dakota Tallman for coordinating much of the research

conducted in 2013, and the many student volunteers who helped with the field and laboratory work.

Literature Cited

Bauer, P., G. Thabeng, F. Stauffer, and W. Kinzelbach. 2004. Estimation of the evapotranspiration rate from diurnal groundwater level fluctuations in the Okavango Delta, Botswana. Journal of Hydrology 288:344–355.

Bauer-Gottwein, P., T. Langer, H. Prommer, P. Wolski, and W. Kinzelbach. 2007. Okavango Delta Islands: interaction between density-driven flow and geochemical reactions under evapo-concentration. Journal of Hydrology 335:389–405.

Bazante, J., G. Jacobi, H. Solo-Gabriele, D. Reed, S. Mitchell-Bruker, D. L. Childers, L. Leonard, and M. Ross. 2006. Hydrologic measurements and implications for tree island formation within Everglades National Park. Journal of Hydrology 329: 606–619.

Bodin, H., A. Mietto, P. M. Ehde, J. Persson, and S. E. B. Weisner. 2012. Tracer behaviour and analysis of hydraulics in experimental free water surface wetlands. Ecological Engineering 49:201–211.

Bouma, T. J., L. A. van Duren, S. Temmerman, T. Claverie, A. Blanco-Garcia, T. Ysebaert, and P. M. J. Herman. 2007. Spatial flow and sedimentation patterns within patches of epibenthic structures: combining field, flume and modelling experiments. Continental Shelf Research 27:1020–1045.

Bowmer, K. H. 1987. Nutrient removal from effluents by an artificial wetland: influence of rhizosphere aeration and preferential flow studied using bromide and dye tracers. Water Research 21:591–597.

Chang, N. B., A. J. Crawford, G. Mohiuddin, and J. Kaplan. 2015. Low flow regime measurements with an automatic pulse tracer velocimeter (APTV) in heterogeneous aquatic environments. Flow Measurement and Instrumentation 42:98–112.

Childers, D. L. 1994. Fifteen years of marsh flumes—A review of marsh-water column interactions in Southeastern USA estuaries. Pages 277–296 *in* W. Mitsch, editor. Global wetlands. Elsevier, Amsterdam, The Netherlands.

Childers, D. L., M. L. Cadenasso, J. M. Grove, V. Marshall, B. McGrath, and S. T. A. Pickett. 2015. An ecology *for* cities: a transformational nexus of design and ecology to advance climate change resilience and urban sustainability. Sustainability 7: 3774–3791.

Childers, D. L., and J. W. Day Jr. 1988. A flow-through flume technique for quantifying nutrient and materials fluxes in microtidal estuaries. Estuarine, Coastal and Shelf Science 27:483–494.

Childers, D. L., and J. W. Day Jr. 1990*a*. Marsh-water column interactions in two Louisiana estuaries. I. Sediment dynamics. Estuaries 13:393–403.

Childers, D. L., and J. W. Day Jr. 1990*b*. Marsh-water column interactions in two Louisiana estuaries. II. Nutrient dynamics. Estuaries 13:404–417.

Childers, D. L., D. Iwaniec, D. Rondeau, G. Rubio, E. Verdon, and C. Madden. 2006. Primary productivity in Everglades marshes demonstrates the sensitivity of oligotrophic ecosystems to environmental drivers. Hydrobiologia 569:273–292.

Childers, D. L., S. T. A. Pickett, J. M. Grove, L. Ogden, and A. Whitmer. 2014. Advancing urban sustainability theory and action: challenges and opportunities. Landscape & Urban Planning 125:320–328.

Daoust, R., and D. L. Childers. 1998. Quantifying aboveground biomass and estimating productivity in nine Everglades wetland macrophytes using a non-destructive allometric approach. Aquatic Botany 62:115–133.

Davis III, S. E., D. L. Childers, J. W. Day Jr., D. T. Rudnick, and F. H. Sklar. 2001*a*. Wetland-water column exchanges of carbon, nitrogen, and phosphorus in a Southern Everglades dwarf mangrove. Estuaries 24:610–622.

Davis III, S. E., D. L. Childers, J. W. Day Jr., D. T. Rudnick, and F. H. Sklar. 2001*b*. Nutrient dynamics in vegetated and unvegetated areas of a southern Everglades mangrove creek. Estuarine, Coastal and Shelf Science 52:753–768.

Fonder, N., and T. Headley. 2010. Systematic classification, nomenclature, and reporting for constructed treatment wetlands. Pages 191–219 *in* J. Vymazal, editor. Water and nutrient management in natural and constructed wetlands. Springer Science + Business Media B.V., Dordrecht, The Netherlands.

Fonder, N., and T. Headley. 2013. The taxonomy of treatment wetlands: a proposed classification and nomenclature system. Ecological Engineering 51: 203–211.

Gendron, P. O., F. Avaltroni, and K. J. Wilkinson. 2008. Diffusion coefficients of several rhodamine derivatives as determined by pulsed field gradient-nuclear magnetic resonance and fluorescence correlation spectroscopy. Journal of Fluorescence 18:1093–1101.

Giraldi, D., M. de'Michieli Vitturi, M. Zaramella, A. Marion, andR. Iannelli. 2009. Hydrodynamics of vertical subsurface flow constructed wetlands: tracer tests with rhodamine WT and numerical modeling. Ecological Engineering 35:265–273.

Greenway, M. 2005. The role of constructed wetlands in secondary effluent treatment and water reuse in subtropical and arid Australia. Ecological Engineering 25:501–509.

Grimm, N. B., S. H. Faeth, N. E. Golubiewski, C. L. Redman, J. Wu, X. Bai, and J. M. Briggs. 2008. Global change and the ecology of cities. Science 319:756–760.

Grove, J. M. 2009. Cities: managing densely settled social-ecological systems. Pages 281–294 *in* F. S. Chapin III, G. P. Kofinas, and C. Folke, editors. Principles of ecosystem stewardship: resilience-based natural resource management in a changing world. Springer, New York, New York, USA.

Harvey, J. W., G. B. Noe, L. G. Larsen, D. J. Nowacki, and L. E. McPhillips. 2011. Field flume reveals aquatic vegetation's role in sediment and particulate phosphorus transport in a shallow aquatic ecosystem. Geomorphology 126:297–313.

Kadlec, R. H., and S. D. Wallace. 2009. Treatment wetlands. Second edition. CRC Press, Boca Raton, Florida, USA.

Kaplan, D., M. Bachelin, R. Munoz-Carpena, and W. Rodriguez-Chacon. 2011. Hydrological importance and water quality treatment potential of a small freshwater wetland in the humid tropics of Costa Rica. Wetlands 31:1117–1130.

Kaplan, D., M. Bachelin, C. Yu, R. Munoz-Carpena, T. L. Potter, and W. Rodriguez-Chacon. 2015. A hydrologic tracer study in a small, natural wetland in the humid tropics of Costa Rica. Wetlands Ecology and Management 23:167–182.

Keefe, S. H., L. B. Barber, R. L. Runkel, J. N. Ryan, D. M. McKnight, and R. D. Wass. 2004. Conservative and reactive solute transport in constructed wetlands. Water Resources Research 40:W01201.

Kjellin, J., A. Worman, H. Johansson, and A. Lindahl. 2007. Controlling factors for water residence time and flow patterns in Ekeby treatment wetland, Sweden. Advances in Water Resources 30:838–850.

Laurent, J., P. Bois, M. Nuel, and A. Wanko. 2015. Systemic models of full-scale Surface Flow Treatment Wetlands: determination by application of fluorescent tracers. Chemical Engineering Journal 264:389–398.

Leonard, L. A., and A. L. Croft. 2006. The effect of standing biomass on flow velocity and turbulence in Spartina alterniflora canopies. Estuarine, Coastal and Shelf Science 69:325–336.

Leonard, L. A., and M. E. Luther. 1995. Flow hydrodynamics in tidal marsh canopies. Limnology and Oceanography 40:1474–1484.

Levenspiel, O. 1998. Chemical reaction engineering. Third edition. Wiley, New York, New York, USA.

Lightbody, A. F., and H. M. Nepf. 2006. Prediction of velocity profiles and longitudinal dispersion in emergent salt marsh vegetation. Limnology and Oceanography 51:218–228.

McLaughlin, D. L., and M. J. Cohen. 2014. Ecosystem specific yield for estimating evapotranspiration and groundwater exchange from diel surface water variation. Hydrological Processes 28:1495–1506.

Melosi, M. V. 2000. The sanitary city: environmental services in urban America from colonial times to the present. Johns Hopkins University Press, Baltimore, Maryland, USA.

Meselhe, E., T. Peeva, and M. Muste. 2004. Large scale particle image velocimetry for low velocity and shallow water flows. Journal of Hydraulic Engineering 130:937–940.

Metson, G., R. Hale, D. Iwaniec, E. Cook, J. Corman, C. Galletti, and D. Childers. 2012. Phosphorus in Phoenix: a budget and spatial representation of phosphorus in an urban ecosystem. Ecological Applications 22:705–721.

Nivala, J., T. Headley, S. Wallace, K. Bernhard, H. Brix, M. van Afferden, and R. A. Müller. 2013. Comparative analysis of constructed wetlands: the design and construction of the ecotechnology research facility in Langenreichenbach, Germany. Ecological Engineering 61:527–543.

Pickett, S. T. A., C. G. Boone, B. P. McGrath, M. L. Cadenasso, D. L. Childers, L. A. Ogden, M. McHale, and J. M. Grove. 2013. Ecological science and transformation to the sustainable city. Cities 32: S10–S20.

Ramberg, L., and P. Wolski. 2008. Growing islands and sinking solutes: processes maintaining the endorheic Okavango Delta as a freshwater system. Plant Ecology 196:215–231.

Sanchez, C. A., D. L. Childers, L. Turnbull, R. Upham, and N. A. Weller. 2016. Aridland constructed treatment wetlands II: Plant mediation of surface hydrology enhances nitrogen removal. Ecological Engineering 97:658–665.

Smart, P. L., and I. M. S. Laidlaw. 1977. An evaluation of some fluorescent dyes for water. Water Resources Research 13:15–33.

Sullivan, P., R. M. Price, F. Miralles-Wilhelm, M. S. Ross, L. J. Scinto, T. W. Dreschel, F. H. Sklar, and E. Cline. 2014. The role of recharge and evapotranspiration as hydraulic drivers of ion concentrations in shallow groundwater on Everglades tree islands, Florida (USA). Hydrological Processes 28: 293–304.

Tanner, C. C., J. P. S. Sukias, T. R. Headley, C. R. Yates, and R. Stott. 2012. Constructed wetlands and denitrifying bioreactors on-site and decentralized water treatment: comparison of five alternative configurations. Ecological Engineering 42:112–123.

Troxler-Gann, T., and D. L. Childers. 2006. Relationships between hydrology and soils describe vegetation

patterns in tree seasonally flooded tree islands of the southern Everglades, Florida. Plant and Soil 279:271–286.

Variano, E. A., D. T. Ho, V. C. Engel, P. J. Schmieder, C. Matthew, and M. C. Reid. 2009. Flow and mixing dynamics in a patterned wetland: kilometer-scale tracer releases in the Everglades. Water Resources Research 45:W08422.

Wallace, S. D., and R. L. Knight. 2006. Small-scale constructed wetland treatment systems: feasibility, design criteria, and O&M requirements. Water Environment Research Foundation (WERF), Alexandria, Virginia, USA.

Weller, N. A., D. L. Childers, L. Turnbull, and R. F. Upham. 2016. Aridland constructed treatment wetlands I: macrophyte productivity, community composition, and nitrogen uptake. Ecological Engineering 97:649–657.

White, W. N. 1932. A method of estimating groundwater supplies based on discharge by plants and evaporation from soil: results of investigations in Escalante Valley, Utah. U.S. Geological Survey Water Supply Paper: 659-A. U.S. Department of the Interior, Geological Survey, Washington, USA.

Williams, C. F., and S. D. Nelson. 2011. Comparison of Rhodamine-WT and bromide as a tracer for elucidating internal wetland flow dynamics. Ecological Engineering 37:1492–1498.

Worman, W., and V. Kronnas. 2005. Effect of pond shape and vegetation heterogeneity on flow and treatment performance of constructed wetlands. Journal of Hydrology 301:123–138.

Supporting Information

Additional Supporting Information may be found online at: http://onlinelibrary.wiley.com/doi/10.1002/ecs2.1756/full